Structural Eng. / Earthquake Eng. Vol. 3. No. 2, 469s-476s. October 1986
Japan Society of Civil Engineers (Proc. of JSCE No. 374/I-6)

AN EXPERIMENTAL STUDY ON SFRC COMPOSITE STEEL DECK

By Hiromasa TERADA, Hirofumi MAENO**, Miyuki NAKAMURA*** and Seichi KOYAMA*****

Composite steel deck system with Steel Fiber Reinforced Concrete (SFRC) has been developed, aiming to improve the durability of deck pavement and the rigidity of steel deck on highway bridges.

The durability of SFRC was clarified through the static and cyclic loading tests using a full scale test bridge, and the measurements were taken on an actual highway bridge in order to confirm its composite effects.

Consequently, it became clear that the structure showed composite behavior with high rigidity not only in floor system but also in main structural system.

Keyword : bridge deck, composite structure, concrete (steel fiber reinforced), field tests

1. INTRODUCTION

The steel deck bridge has such characteristic as high load carrying capacity, and has been widely used to geometrically restricted structures at city areas in Japan. On the orthotropic steel deck of these bridges, bituminous concrete is usually used for pavement. It is light in weight, easy to treat, but weak in temperature changes. Those features, however, give rise to the problems such as flow, cracking, and separation from the steel deck.

Also these problems havs sometimes caused the undesirable vibration in bridges, which resulted in a discomfort to drivers and fatigue damages to bridge members.

In the past decade, the concrete containing discrete randomly dispersed small steel fibers (SFRC) has been used for tunnel lining, airport pavement, roadway slab and so on. The introduction of fibers into the concrete matrix imparts to certain characteristics of concrete such as resistance to spalling, capability of sustaining load and keeping cracks tightly closed after cracking. Thus, it is expected that SFRC on the steel deck improves its stability as pavement and at the same time rises the rigidity of steel deck due to the composite effect.

In this paper, two cases of SFRC composite steel deck are examined. One involves the investigation about the composite behaviors based on a full scale modelled test bridge under static and cyclic loading tests. The other is the measurements on the two span continuous curved bridge in order to confirm the applicability of this structural system for standard use.

* Member of JSCE, Research Institute, Yokogawa Bridge Works, LTD. (Shinminato 88, Chiba 260)
** Member of JSCE, Nagoya Expressway Public Corporation (Marunouch 1-16-15, Naka-ku, Nagoya 460)
*** Member of JSCE, Sumitomo Heavy Industories, LTD. (Natsushima-cho 19, Yokosuka 237)
**** Member of JSCE, Central Research Laboratories Sumitomo Metal Industories, LTD. (Sunayama 16, Hasaki-cho, Ibardgi 314-04)

2. FIELD TEST ON MODEL BRIDGE

(1) Description of model bridge

Previous to the application of SFRC composite steel deck to practical use, field test on a modelled bridge was carried out. The model bridge shown in Fig. 1 consists of three main girders and composite deck. The span length is 8 m and the total width 5.6 m. This bridge was designed by the allowable stress approach according to Specifications for Highway Bridges in Japan[1], where the design load TL-20 adopted in this test is prescribed in such way that rear wheel load is 8 000 kg, total weight 20 000 kg and impact coefficient 0.4.

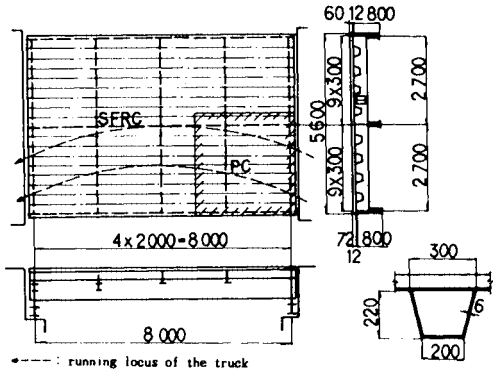

Fig. 1 Modelled Bridge Configurations.

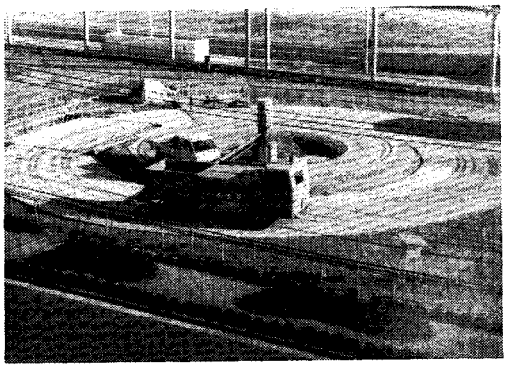

Photo 1 Test Apparatus.

SFRC cast in place was 60 mm and 72 mm thick as shown in Fig. 1, and plain concrete was also cast in a portion of the deck in order to compare its cracking behavior with that of SFRC under cyclic loading.

Each mix for SFRC and plain concrete are shown in Table 1. The expand mixture was included for the purpose of controlling shrinkage. The fibers were of the shearing type with a cross section of 0.5 mm× 0.5 mm and 30 mm long. Concrete batched at a ready-mix facility was carried to the site by the transit-mix truck and was placed on the bridge, then followed stricking off, vibrating and smooth finishing.

The shear connectors were of stud bolt type of 9.5 ϕ×40 mm.

Table 1 Concrete Mixes.

Concrete type	Air (%)	Slump (cm)	S/A (%)	W/C (%)	S.F (vol.%)	Unit weight (kg/m³)						
						W	C	S	G	SF	AE	E.A
SFRC	5.0	5.0	70	50	1.5	220	390	1103	466	118	1.027	50
PC	4.2	6.0	42.3	50		158	286	789	1065		0.794	30

AE : AE agent, E. A : Expansive admixture, S/A : Sand-Aggregate ratio

(2) Test apparatus

The applied test apparatus has been constructed for road endurance tests with a 12 m running radius of a test truck and 6 m effective width. The model bridge was mounted on the pit which was provided for this test. The test truck with an electrically driven motor varies its speed from 5 km/h to 30 km/h and the total weight varies from 9 250 kg to 20 000 kg by loading.

The test apparatus is shown in Photo 1. The bridge is set as the outer rear wheel of the truck runs the center of the bridge (see Fig. 1).

(3) Test procedure

Prior to concrete casting, the first static loading test was carried out in a state of steel deck using 15 000 kg truck weight (rear wheel load : 5 000 kg) in order to get the comparative data with that of composite deck.

After stud welding, concrete casting and its curing with wet membrane for over four weeks, the second static loading test was executed under the same truck load. Uninterruptedly, the running loading test was carried out at 2×10^5 cycles with the truck. This means that if there are initial latent cracks, they must reveal themselves under the cyclic loading.

The inspection of the concrete surface showed no damage, and the third static loading test and measurment were carried out under the incresed truck weight of rear wheel load to 8 000 kg.

After that, the second running loading of 2×10^5 cycles with a total weight of 15 000 kg was practiced again. In this test, no cracks were aleoobserved and the fourth loading test was carried out using the 29 000 kg tandem axles truck.

At each static test, strains, deflections and the others were measured by use of such instruments as electrical resistance gages, electrical deformation measuring devices, contact gages, etc. At the same time, visual inspections of concrete surface were performed.

Calculated values for ribs are evaluated from grid structure system composed of main girders, transverse ribs and longitudinal ribs. Those for deck plate are from FEM analysis. The effective widths of each member are based on the prescribed methods in Reference 1) and elastic modulus ratio is assumed as $n=E_s/E_c=7$.

(4) Test results

Overall the model bridge retaind its original configuration during a long time test period.

No cracks of SFRC were observed even at the end of the tests. In plain concrete pavement, a crack developed first at the edge on the interior main girder at the third static loading.

During the second running test, this crack propagated to the direction of the span center along a continuous line and stopped at the boundary between plain concrete and SFRC.

Test result are shown in Figs. 2, 3 and 4.

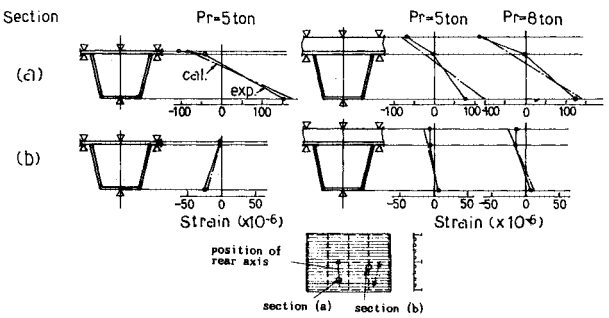

Fig. 2 Strain Distributions in Longitudinal Rib.

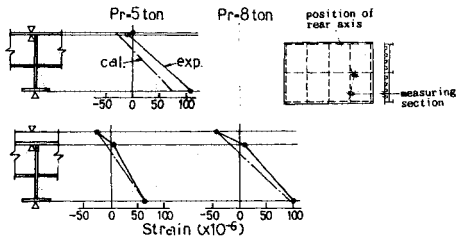

Fig. 3 Strain Distributions in Transverse Rib.

Fig. 2 shows the strain distributions in longitudinal ribs, in which section (a) is that of maximum moment region and section (b) of minimum moment region. At section (b) of negative moment region, a considerable difference between non-composite and composite state is recognized.

The slope of strain distribution varies from that of negative moment at non-composite state to that of positive moment at composite state. Moreover, the strain distribution at each loading step is proportional to the load intensity. It may be, therefore, concluded that, by the increment of flexural rigidity of plate and longitudinal ribs due to the composite effect, deck structure indicates such behavior as an orthotropic plate and that composite action is kept in good condition after cyclic loadings.

Fig. 3 shows the strain behavior of a transverse rib. The strain measuring location is at near span center of the transverse rib and the wheel rear axle is on the rib. In the non-composite state, measured strain distribution differs a little from that of the calculation based on a grid-structure system. This may be because of the low flexural rigidity of steel deck plate under direct loading. On the contrary, in the

composite state the tendency of strain distribution is similar on both measured and calculated strains at each loading step.

Therefore, it may be clear that the structural system of transverse rib behaves as a composite section.

Fig. 4 shows a typical strain distributions in deck plate. Fig. 4(a) is for the transverse strain distribution of the plate surface near interior main girder for both non-composite and composite states. Fig. 4(b) is for the longitudinal strain distribution near transverse rib. The magnitude and distribution of the strains in plates considerably vary according to whether concrete is cast or not.

In the composite state, strain distribution becomes uniform, and excess tensile and compressive strains in plates disappear. This is due to the increment of flexural rigidity of the plate by the composite effect and may be efficient for the prevention of such fatigue cracking that is now world-widely in problem.

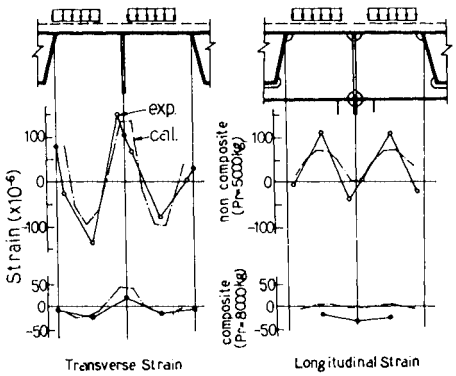

Fig. 4 Strain Distribution in Deck Plate.

3. FIELD TEST ON PRACTICAL BRIDGE

(1) Description of the bridge

The bridge provided with SFRC pavement is shown in Fig. 5. This is located at the off-ramp of a highway in Nagoya District and has the small curvature as $R=35$ m because of the restriction due to geographical feature.

The longitudinal slope is about 3 % and the transverse slope is max. 10 %, which bring the pavement under severe condition by the vehicle loads. Originally SFRC is designed as pavement and is not considered to be composite structure in practice. However, surface strains on a steel deck plate are limited less than 150×10^{-6} at the root of brackets in order to prevent the crack occurence in SFRC.

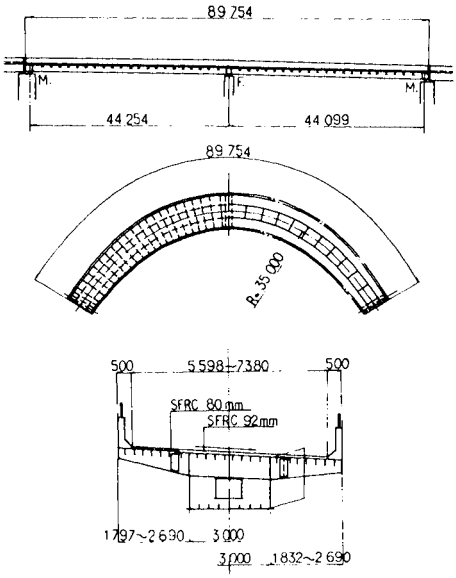

Fig. 5 Tested Bridge with SFRC Pavement.

Table 2 Design Conditions.

Design compressive strength	300 kg/cm²
Combined strength	345 kg/cm²
Max. size coarse aggregate	15 mm
Slump	8±2.5 cm
Water-cement ratio	> 50 %
Air content	4±1 %
Fiber content	1.5 vol.%
Expand admixture content	30 kg/m³

a) Design of SFRC

SFRC was designed in accordance with the Design Specification on Pavement 1984 by Nagoya Expressway Public Corporation[2]. This Specification provides that SFRC is applied in such cases as the bridge with large longitudinal or transverse slope, where the mastic asphalt pavement is difficult to be applied, and the bridge under considerable traffic congestion at on- and off-ramp.

The design condition applied is shown in Table 2. This is almost same to that of the model bridge and the fibers used are of stainless steel of SUS 304 in order to aboid the dirt by rust on SFRC surface. Shear connectors were arranged at 25 cm pitch at ordinary portions and 20 cm pitch near end supports in the longitudinal direction, which was decided by the shearing force between SFRC and the main girder system. In the transverse direction, shear connectors were arranged at 25 cm standard pitch. The size of shear connector is $9.5\,\phi\times40$ mm long of bolt type.

b) Construction of SFRC

As the total width of the bridge varies from 5.6 m to 7.38 m at the sections, SFRC was placed at two stages. First, the both shoulders of the road with 0.899 m to 1.79 m width each were constructed by manual works. After the curing in one week, the central part of 3.8 m width was constructed by mechanical works. At the positions of joint and at the interior support region, wire mesh was provided in order to prevent cracking.

Photo 2 shows the casting of SFRC.

(2) Loading test

In the same manner as the test on the model bridge, loading tests were carried out in both states of non-composite and of composite. Using six trucks of 20 tonf weight, the measurements of deflection and strains were taken in the main girder and the deck panels.

At the same time, vibration responses were measured using acceleration equipment at both states. Measuring of deflection was realized by the water level method using 5 ϕ continuous vinyle pipe for the main girder and by the electrical deflection meters for the deck panel. For strain measurements, strain gages were used. Fig. 6 shows the loading cases, loading truck positions and measuring positions.

Photo 2 Casting of SFRC.

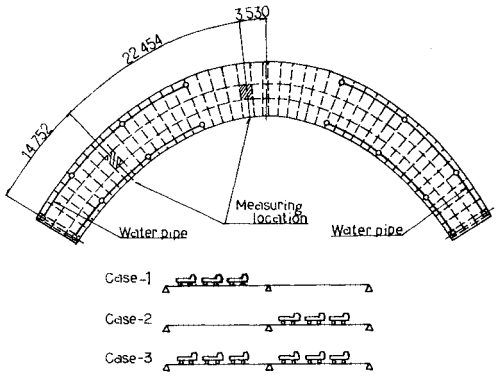

Fig. 6 Loading Cases and Measuring Locations.

(3) Test results

a) Main girder

Measured deflections of the main girder are shown in Fig. 7 for each loading case.

The flexural rigidity rises according to the composite effect. The comparison between measured and calculated deflection is shown in Table 3, in which the deflection of composite state is calculated as a composite girder with Young's modulus ratio $n=E_s/E_c=7$.

Since the measured deflections are similar to those of calculation, it is clear that the main girder behaves almost as a composite structure. In Fig. 8, the stress distributions are shown for both non-composite and composite states. The measured stress distributions in composite state agree with the calculated results at both negative moment and positive moment regions. At the same time, the stresses at upper and lower flange plates are nearly constant at any positions and the effects of shear lag or warping torsion have little influence.

The result of vibration test is shown in Fig. 9. The vertical axis is a deflection amplitude in log and the horizontal axis is the number of vibration waves at free vibration. The logarithmic decrement of 0.0725 in non-composite state changed to 0.113 at composite state. This may be an excellent characteristic of SFRC composite structure.

Table 4 shows the comparison of natural frequencies in bending vibration, where the contribution of the rigidity of the wall-type guardrails and SFRC is taken as parameters.

The measured frequencies are close to such case that there is the contribution of both rigidities.

Table 3 Comparison of Deflection in Main Girder.

Item \ Deflection		Loading cases Case-1	Case-2	Case-3
non-composite state	Cal.①	16.5	16.7	7.4
	Cal.②	10.9	11.0	4.7
	Exp.③	13.6	13.7	6.6
	①/③	1.27	1.22	1.12
	②/③	0.80	0.80	0.71
composite state	Cal.④	13.4	13.7	6.0
	Cal.⑤	8.8	9.1	3.7
	Exp.⑥	10.7	10.8	4.8
	④/⑥	1.25	1.27	1.25
	⑤/⑥	0.82	0.84	0.77
③/⑥		1.27	1.27	1.38

Unit : mm
Cal.①,④ : without wall, Cal.②,⑤ : with wall
Exp.③,⑥ : measured deflection in each state

Table 4 Comparison of Natural Frequency.

Item \ Frequency			Analysis wall	Analysis without wall	Experiment
before casting		f_1	2.370	1.968	2.17~2.35
		f_2	3.244	2.032	3.23~3.90
after casting	composite	f_1	2.344	1.943	
		f_2	3.042	2.087	f_1=2.15~2.37
	non-composite	f_1	2.124	1.762	f_2=3.23~3.73
		f_2	2.903	1.818	

unit : Hz

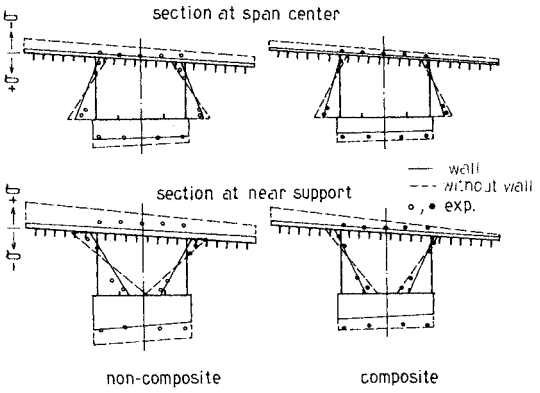

Fig. 8 Stress Distribution in Main Girder.

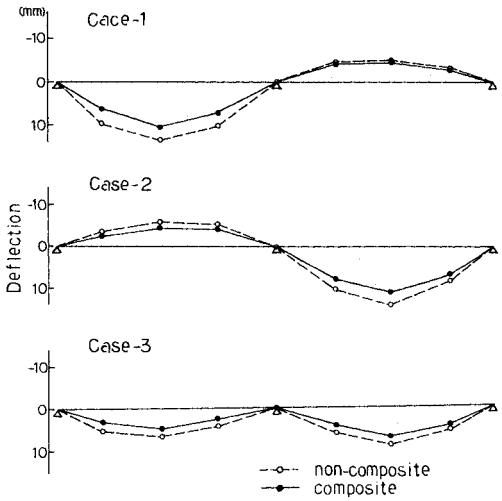

Fig. 7 Measured Deflection Curves.

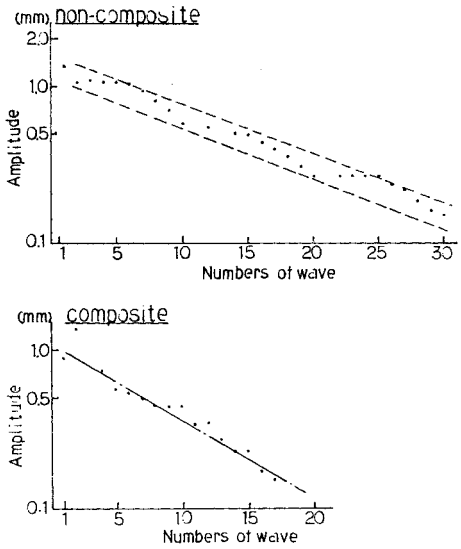

Fig. 9 Relationship between Amplitude and Numbers of Wave.

b) Deck structure

The analytical model is shown in Fig. 10, in which the two panels of deck structure divided by diaphragms are modelled as an orthotropic plate. Longitudinal ribs and transverse ribs are taken as beam elements, while the effective width of deck plates derived from Specification for Highway Bridges in Japan is assumed to be the same at both non-composite and composite states. The properties of members in the calculation are listed in Table 5. The bending rigidity at composite state improves by 129 times compared at non-composite state in the deck plate, 1.61 times in the longitudinal rib and 1.20 in the transverse rib, respectively. Because the degree of improvement is higher in small sectional members such as the deck plate than in the large members, the composite effect may be remarkable in the small sectional members.

The diagrams of bending moment in a transverse rib and longitudinal ribs, which are calculated from measured strains and sectional constants, are shown in Figs. 11 and 12, respectively. Since the measured ones are similar to the analytical values in both non-composite and composite states and the bending moments at the composite states are lower than in non-composite state, it is evident that the analytical

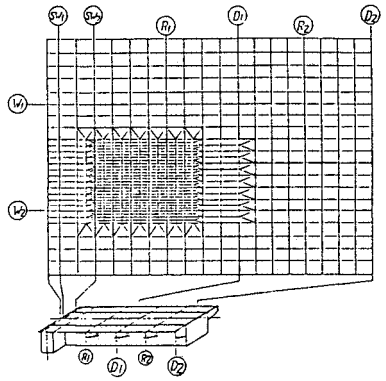

Fig. 10 Analytical Model.

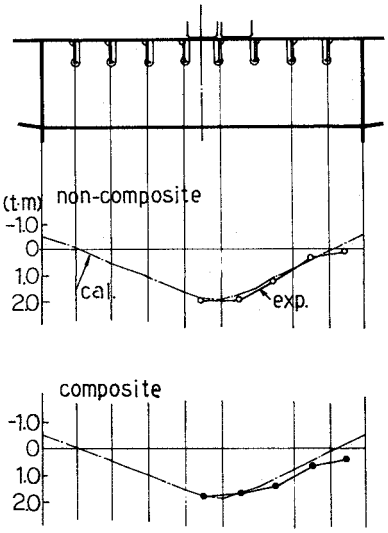

Fig. 11 Bending Moment Diagram in Transverse Rib.

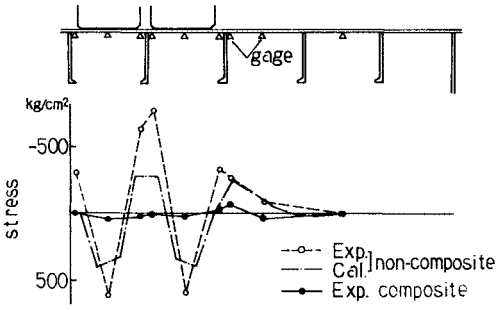

Fig. 13 Stress Distribution in Deck Plate.

Table 5 Moment of Inertia in Calculation.

unit : Hz

member	non-composite	composite	ratio
deck plate	0.144	18.624	129
long. rib	4 761	7 678	1.61
trans.rib	217 014	261 345	1.20

unit : cm^4

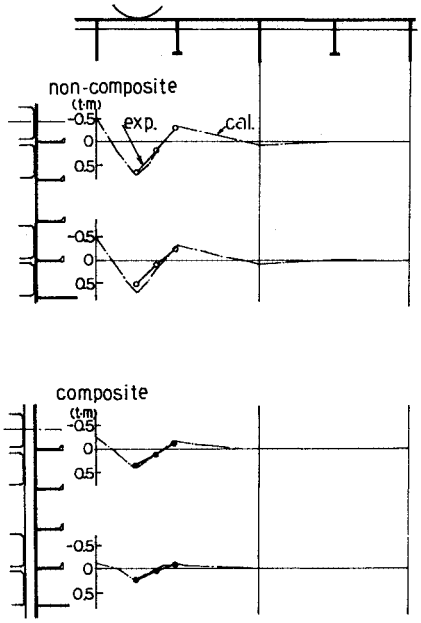

Fig. 12 Bending Moment Diagram in Longitudinal Ribs.

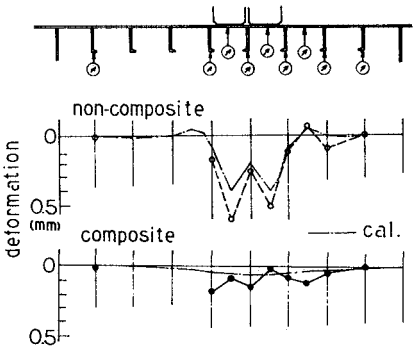

Fig. 14 Deformation in Cross Section.

model is appropriate and members behave themselves like composite structures.

Next, the behaviors of the plate are shown in Figs. 13 and 14. Fig. 13 shows the stress distribution in the deck plate in the transverse direction, which is arranged by the measured values at the lower surface. The stress distribution is considerably normalized after composing and the local bending in non-composite state diminishes. This tendency results from the increment of plate stiffness accompanying to the composite effect and agrees with the result in the model bridge shown in Fig. 4.

Fig. 14 shows the deformation of a cross section under wheel loading. The deformation in non-composite state is different from that in composite state in such a way that the former shows the large deflection at the center of plate pannel, while the latter shows the comparatively smooth shape as a whole. For reference, the deformation diagrams in the analysis are shown in Fig. 15. This result is similar to the contents of Fig. 13 and 14. It is, therefore, concluded that the deck structure is altered from the grid-type structural system in non-composite state to the plate-type structural system in the composite state. Here, the dispersion of the measured data in composite state seems to arise from the measuring error because of the little values such as 0.1 mm.

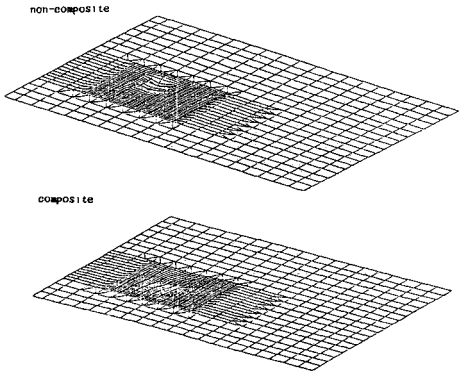

Fig. 15 Analytical Result on Deformation of Deck Structure.

4. SUMMARY AND CONCLUDING REMARKS

Presented in this paper are the results of two experimental studies carried out on SFRC composite steel deck bridges. The main conclusions may be summarized as follows;

① Any damage did not occure at the suface of SFRC on model bridge, while in the plain concrete cast in a part on the bridge in order to compare cracking behavior with SFRC, a surface crack was observed on the interior main girder at fifty thousand cycles of traffic loading. Also, the deck members composed of SFRC showed the behavior as composite structure even after one million cycles of traffic loading.

② In particular, the flexural rigidity of plate increased considerably by the composite effect. As the result, the deck structure composed of a composite plate, longitudinal ribs and transverse ribs behaved as the orthtropic plate system with the normalization of locally exceeded strains and deformation.

This structural system was, therefore, confirmed to be applied to the practical uses.

③ Then followed the loading test on the two span continuous composite bridge in Nagoya Expressway. On the main girder, the flexural rigidity in composite state increased 25~30 % in comparison to the non-composite state. But it could not be confirmed in calculation because the influence of wall-type guardrails and the effective width were not clear.

The natural frequency in the vibration test showed nearly the same results between two states, but as for the structural damping, the damping ratio in composite state exceeded that at non-composite state by 50 %

④ On the deck structure, the test results were generally consistent with the analytical ones at both states. Moreover, SFRC and steel deck structure showed the whole composite behavior, resulting in the decrement of local deformation and stresses and also the increment of flexural rigidity. These agreed with the results on the model bridge.

⑤ Consequently, this composite deck system may be applicable widely to practical uses.

In future, it may be possible to reduce the thickness of steel plate and to widen the spacing of longitudinal ribs.

REFERENCES

1) Japanese Road Association : Specifications for Highway Bridges (JSHB), Feb. 1980.
2) Nagoya Expressway Public Corporation : Design Specifications for Pavement, Aug. 1984.

(Received November 8 1985)